NUCLEAR DATA AND MEASUREMENTS SERIES

ANL/NDM-135

Neutron Scattering from Elemental Uranium and Thorium

by

A.B. Smith and S. Chiba

January 1995

ARGONNE NATIONAL LABORATORY,
ARGONNE, ILLINOIS 60439, U.S.A.

NUCLEAR DATA AND MEASUREMENTS SERIES

ANL/NDM-135

NEUTRON SCATTERING FROM ELEMENTAL URANIUM AND THORIUM

A. B. Smith and S. Chiba

January, 1995

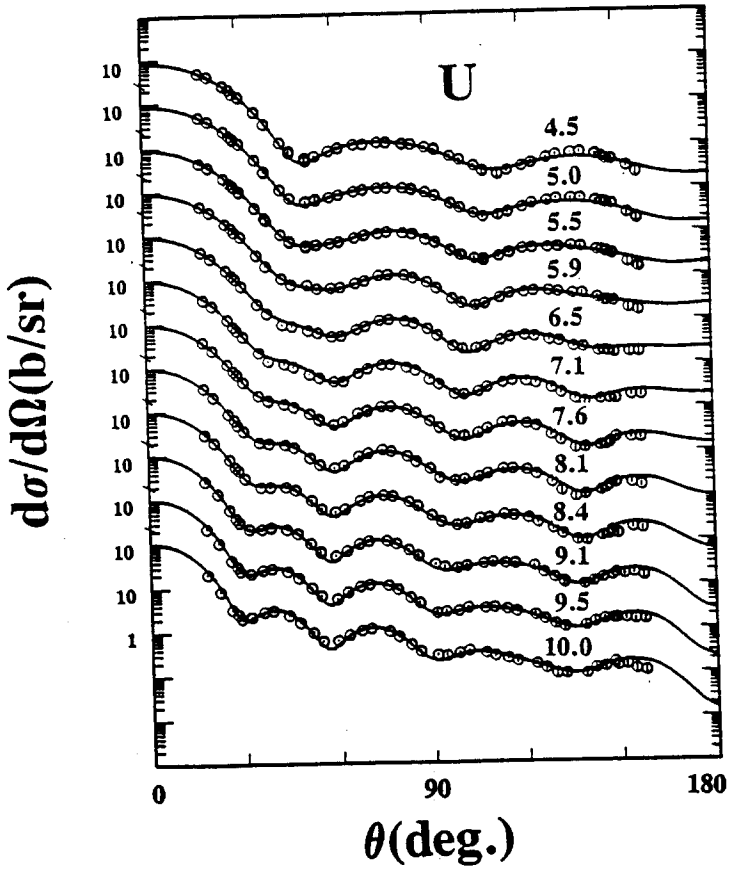

ARGONNE NATIONAL LABORATORY, ARGONNE, ILLINOIS
Operated by THE UNIVERSITY OF CHICAGO
for the U. S. DEPARTMENT OF ENERGY
under Contract W-31-109-Eng-38

Argonne National Laboratory, with facilities in the states of Illinois and Idaho, is owned by the United States government, and operated by The University of Chicago under the provisions of a contract with the Department of Energy.

DISCLAIMER

This report was prepared as an account of work sponsored by an agency of the United States Government. Neither the United States Government nor any agency thereof, nor any of their employees, makes any warranty, express or implied, or assumes any legal liability or responsibility for the accuracy, completeness, or usefulness of any information, apparatus, product, or process disclosed, or represents that its use would not infringe privately owned rights. Reference herein to any specific commercial product, process, or service by trade name, trademark, manufacturer, or otherwise, does not necessarily constitute or imply its endorsement, recommendation, or favoring by the United States Government or any agency thereof. The views and opinions of authors expressed herein do not necessarily state or reflect those of the United States Government or any agency thereof.

Reproduced from the best available copy.

Available to DOE and DOE contractors from the
Office of Scientific and Technical Information
P.O. Box 62
Oak Ridge, TN 37831
Prices available from (615) 576-8401

Available to the public from the
National Technical Information Service
U.S. Department of Commerce
5285 Port Royal Road
Springfield, VA 22161

ANL/NDM-135

NEUTRON SCATTERING FROM ELEMENTAL URANIUM AND THORIUM*

by

A. B. Smith[a,b] and S. Chiba[c]

[a] Argonne National Laboratory
Argonne, Illinois

[b] The University of Arizona
Tucson, Arizona

[c] Japan Atomic Energy Research Institute
Tokai-mura, Naka-gun, Ibaraki-ken, Japan

January, 1995

Keywords:

Measured Neutron Scattering from Elemental Uranium and Thorium, 4.5 - 10 MeV. Coupled-channels Model Interpretations. Comparisons with ENDF/B-VI.

---

* This work supported by the U. S. Department of Energy under Contract No. W-31-109-ENG-38; and by the Department of Nuclear and Energy Engineering, The University of Arizona.

Technology Development Division
Argonne National Laboratory
9700 South Cass Avenue
Argonne, Illinois 60439
U. S. A.

PUBLICATIONS IN THE ANL/NDM SERIES

A listing of recent issues in this series is given below. Issues and/or titles prior to ANL/NDM-118 can be obtained from the National Technical Information Service, U. S. Department of Commerce, 5285 Port Royal Road, Springfield, VA 22161, or by contacting the author of this report at the following address:-

Technology Development Division
Argonne National Laboratory
9700 South Cass Avenue
Argonne, IL 60439
USA

J.W. MEADOWS
Characteristics of the Samples in the FNG Fission Deposit Collection
ANL/NDM-118 (November 1990)

S. CHIBA, P.T. GUENTHER, A.B. SMITH, M. SUGIMOTO, AND R.D. LAWSON
Fast-Neutron Interaction with Elemental Zirconium, and the Dispersive Optical Model
ANL/NDM-119, June 1991

A.B. SMITH, P.T. GUENTHER, J.F. WHALEN, AND S. CHIBA
Fast-neutron Total and Scattering Cross Sections of ^{58}Ni and Nuclear Models
ANL/NDM-120, July 1991

S. CHIBA AND D.L. SMITH
A Suggested Procedure for Resolving an Anomaly in Least-squares Data Analysis Known as "Peelle's Pertinent Puzzle" and the General Implications for Nuclear Data Evaluation
ANL/NDM-121, September 1991

D.L. SMITH AND DOMINIQUE FEAUTRIER
Development and Testing of a Deuterium Gas Target Assembly for Neutron Production Via the H-2(D,N)HE-3 Reaction at a Low-energy Accelerator Facility
ANL/NDM-122, March 1992

D.L. SMITH AND E.T. CHENG
A Review of Nuclear Data Needs and Their Status for Fusion Reactor Technology with some Suggestions on a Strategy to Satisfy the Requirements
ANL/NDM-123, September 1991

J.W. MEADOWS
The Thick-Target $^{9}Be(d,n)$ Neutron Spectra for Deuteron Energies Between 2.6 and 7.0-MeV
ANL/NDM-124, November 1991

A.B. SMITH AND P.T. GUENTHER
Fast-Neutron Scattering Near Shell Closures:- Scandium
ANL/NDM-125, August 1992

A.B. SMITH, J.W. MEADOWS AND R.J. HOWERTON
A Basic Evaluated Neutronic Data File for Elemental Scandium
ANL/NDM-126, November 1992

A.B. SMITH AND P.T. GUENTHER
Fast-Neutron Interaction With Vibrational Cadmium Nuclei
ANL/NDM-127, November 1992

D.L. SMITH
A Least-Sqeares Computational "Tool Kit"
ANL/NDM-128, April 1993

JOSEPH McCABE, A.B. SMITH AND J.W. MEADOWS
Evaluated Nuclear Data Files for the Naturally-Occuring Isotpes of Cadmium
ANL/NDM-129, June 1993

A.B. SMITH AND P.T. GUENTHER
Fast-Neutron Interaction with the Fission Product ^{109}Rh
ANL/NDM-130, September 1993

A.B. SMITH AND P.T. GUENTHER
Fast-Neutron Scattering from Vibrational Palladium Nuclei
ANL/NDM-131, October 1993

A.B. SMITH
Neutron Interaction with Doubly-Magic ^{40}Ca
ANL/NDM-132, December 1993

A.B. SMITH
Fast-Neutron Scattering at Z = 50:- Tin
ANL/NDM-133, September 1994

A.B. SMITH, S. CHIBA AND J.W. MEADOWS
An Evaluated Neutronic Data File for Elemental Zirconium
ANL/NDM-134, September 1994

TABLE OF CONTENTS

Abstract---------- 1

I. Introduction---------- 2

II. Experimental Methods---------- 3

III. Experimental Results---------- 5

IV. Coupled-Channels Models---------- 6

V. Discussion---------- 15

References---------- 27

ANL/NDM-135

NEUTRON SCATTERING FROM ELEMENTAL URANIUM AND THORIUM

by

A. B. Smith and S. Chiba

ABSTRACT

Differential neutron-scattering cross sections of elemental uranium and thorium are measured from ≈ 4.5 to 10.0 MeV in steps of ≈ 0.5 MeV. Forty or more differential values are obtained at each incident energy, distributed between ≈ 17^{o} and 160^{o}. Scattered-neutron resolutions are carefully defined to encompass contributions from the first four members of the ground-state rotational band (0^{+} g.s., 2^{+}, 4^{+} and 6^{+} states). The experimental results are interpreted in the context of coupled-channels rotational models, and comparisons made with the respective ENDF/B-VI evaluated files. These comparisons suggest some modifications of the ENDF/B-VI ^{238}U and ^{232}Th evaluations.

I. INTRODUCTION

For more than a quarter of a century the inelastic neutron-scattering processes in the fertile nuclei ^{232}Th and ^{238}U have been a significant concern in fast fission-reactor physics [YOM60]. These processes are major energy-transfer mechanisms in the blankets of fast-reactor systems thereby influencing neutron economy, safety, breeding ratios, and other system neutronic parameters. In the beginning it was not technologically possible to explicitly measure the respective discrete inelastic-scattering cross sections, and recourse was made to broad-resolution determinations of elastic- and nonelastic-scattering processes [BWS56]. The results, corrected for fission-neutron contributions, gave some indication of the magnitude of the inelastic-scattering processes. The technological situation considerably improved with the advent of the fast-neutron time-of-flight technique [CL55]. This method has been widely exploited over a number of years to obtain the cross sections for the inelastic-neutron excitation of states in ^{232}Th and ^{238}U at low incident energies (e.g., see refs. [Smi63], [Bar+66], [Ega+88] and [Hao+82]). Both nuclei are collective rotors, with the first few excited states members of the ground-state rotational band (0^+ g.s., 2^+ $E_x \approx 50$ keV, 4^+ $E_x \approx 150$ keV and 6^+ $E_x \approx 330$ kev) [NDS]. Above ≈ 650 keV a complex of excited states appears due to components of β- and γ-vibrational bands, and above ≈ 1 MeV the density of excited levels increases very rapidly with energy. The fundamental nature of these higher-lying levels is not certain. This complexity makes it increasingly difficult to measure the respective inelastic-scattering cross sections, and the lack of detailed physical understanding seriously compromises calculational estimates based upon compound-nucleus or direct-reaction nuclear models. Above ≈ 3.5 MeV incident-neutron energies there are no explicit experimental determinations of ^{232}Th and ^{238}U discrete inelastic-scattering cross sections, and the few continuum neutron-emission measurements available are seriously compromised by fission and (n,2n) neutron contributions. Thus, at higher energies evaluated data sets (e.g., ENDF/B [ENDF]) used in applications are generally based upon estimates deduced from nonelastic cross sections, and even these are compromised by the lack of detailed elastic-scattering measurements. Such elastic-scattering results as are available (e.g., [Kni+71], [BGT+65] and [Han+86]) tend to lack the detail requisite for quantitative interpretation, and some are many decades old.

It is now possible to provide comprehensive and accurate cross sections for scattering from the ^{238}U and ^{232}Th ground-state-rotational bands; i.e., differential cross sections

for the combined scattering from the 0^+, 2^+, 4^+ and 6^+ levels of the band. At the same time, application of calculational methods has improved to the point where the results of careful composite scattering measurements can be explicitly fitted using coupled-channels methods in a manner that suggests better understanding of the individual components of the measured cross sections and their distributions with angle ([Tam65], [Ray79] and [Mol81]). Thus, there is now a potential for an improved knowledge of the elastic-scattering cross sections and those of the low-lying inelastic excitations over a wide energy range, which, together with the well established total cross sections [ENDF], defines the non-elastic cross section to several percent [SGM82]. The non-elastic cross section primarily consists of inelastic-scattering, fission and (n,2n) contributions. Since the latter two components are reasonably well known and/or small (or non-existent at many energies), an improved determination of the total inelastic-scattering cross section is possible.

The goal of the present measurements and associated interpretations was improved knowledge of the elastic, ground-state rotational-band inelastic and the total-inelastic scattering cross section of ^{232}Th and ^{238}U for incident energies of ≈ 4 to 10 MeV. The experimental method is described in Section II. The experimental results are given in Section III, and their interpretations using coupled-channels models are given in Section IV. The results are discussed in Section V, including comparisons with comparable values taken from ENDF/B-VI.

II. EXPERIMENTAL METHOD

The measurements were made using the time-of-flight method and the Argonne multi-detector system [Smi+67]. It is technologically impracticable to experimentally resolve the differential scattering cross sections for the excitation of the components of the ground-state-rotational band of either ^{232}Th or ^{238}U at the incident-neutron energies of the present experiments. Therefore, the measurements determined the differential cross sections for the composite excitation of the 0^+ g.s., 2^+, 4^+ and 6^+ levels of the ground-state rotational band.

The neutron source used in the measurements was the D(d,n) reaction [Dro87], with the target deuterium gas contained in a cell 2 cm long. The pressure of the gas in the cell was adjusted so that the neutron energy spread from the source at a zero-degree reaction angle varied from ≈ 250 keV to ≈ 120 keV as the neutron energy increased from 4.5 to 10 MeV. The mean neutron energy was determined to within ≈± 50 keV by control of the energy of the incident deuteron beam. The source was pulsed at a repetition rate of 2 MHz, with a burst duration of ≈ 1 nsec. The source intensity was monitored using a time-of-flight system

located at an ≈ 5^{o} reaction angle and with a flight path of ≈ 7 m.

The measurement samples were solid metal cylinders 2 cm in diameter and 2 cm long, placed 16 cm from the neutron source at a zero-degree source-reaction angle. The neutrons were incident upon the lateral surfaces of the samples. The uranium and thorium samples were fabricated of elemental metal of better than 99.9% chemical purity. The ≈ 0.75% contribution of the minor isotopes in the uranium sample was ignored throughout this work as it would have distorted the measured results by amounts less than the experimental uncertainties (i.e., natural uranium was assumed to be entirely ^{238}U).

A heavy shield defined ten flight paths with lengths of 500 to 503 cm distributed over scattering angles of ≈ 17^{o} to 160^{o}. These flight paths, and the above-cited burst durations, provided velocity resolutions sufficient to resolve the ground-state rotational-band from other scattering components. The collimator system was varied over four or more angular increments thereby providing at least 40 differential measurements at each incident energy. The determination of the scattering angles was a critical matter as the angular distributions are very forward peaked. The relative angular scale was optically determined to $\leq 0.1^{o}$. The normalization of this relative scale was accomplished by scattering neutrons at forward angles, both left and right of the apparent center line, where the cross sections are changing very rapidly with angle. These latter calibrations were repeated at each incident energy and measurement period with results that were believed known to $\leq 0.1^{o}$. This conclusion was supported by reproducibility.

The scattered-neutron detectors were 12 cm diameter and 2 cm thick cylindrical liquid hydrogenous scintillators, placed at the ends of the respective flight paths. Their relative energy-dependent responses were determined by the observation of neutrons emitted at the fission of ^{252}Cf using the method described in ref. [SGS77]. These relative detector efficiencies were normalized to the well known H(n,n) standard cross section [CSL83] by observing neutron scattering from CH_2 at a 30^{o} scattering angle. Detector γ-ray response was suppressed with pulse-shape-sensitive circuitry.

The multi-parameter data was accumulated in a digital computer system and analyzed off-line using an integrated data-processing system developed over many years [SG90]. The observed velocity spectra were carefully analyzed to assure that the cross sections included contributions from the $0^{+} \rightarrow 6^{+}$ components of the ground-state rotational band, and excluded

inelastic-scattering contributions from higher-lying levels (e.g. from β- and γ-vibrational bands). The observed velocity spectra included a fission and (n,2n) neutron contribution underlying the neutron-scattering component of interest. The primary spectral interpretation located regions respectively above and below the scattered-neutron peak of interest, determined the fission and (n,2n) component at these either extremes, and linearly interpolated and subtracted the contribution under the scattering peak. A secondary approach simply summed the scattered-neutron and continuum contributions between the two limits to determine the "emission" contribution, and then subsequently subtracted the fission-neutron and (n,2n) components as outlined below. The two approaches were applied to the same velocity spectra.

The "raw" cross sections were corrected for multiple-event, beam-attenuation and angular-resolution effects using Monte-Carlo procedures [Smi90]. These corrections were applied to both the H(n,n) standard and the uranium and thorium measurements. The Monte-Carlo calculations were iterated three times to assure a reasonable convergence.

III. EXPERIMENTAL RESULTS

The measurements were made at incident energies of ≈ 4.5 to 10 Mev in steps of ≈ 0.5 MeV. The scattered-neutron resolution was set at ≈ 0.4 MeV so as to include the 0^+ g.s., 2^+, 4^+ and 6^+ levels of the ground-state rotational band in the measured distributions. The differential cross-section uncertainties ranged from ≈ 3% in regions of large cross section to larger values at the minima of the distributions. These uncertainties included statistical effects and estimates of systematic contributions due to; detector normalizations, correction procedures, angle uncertainties, and resolution effects. The uranium and the thorium results are summarized in Figs. III-1 and III-2, respectively. The measured values at each incident energy were fitted with Legendre-polynomial expansions to obtain the angle-integrated cross sections, including considerations of Wick's Limit [Wic43]. The results of these fitting procedures are indicated by the curves in Figs. III-1 and III-2. The resulting angle-integrated values were compared with the comparable quantities given in ENDF/B-VI, as indicated in Figs. III-3 and III-4. The illustrated uncertainties on the experimental angle-integrated values are subjective estimates of the goodness of the fitting procedures. Fig. III-1 through III-4 are relevant to the scattering cross sections. The emission cross sections were treated in an identical manner and corrected for fission and (n,2n) contributions to provide a comparison with the scattering results. The corrections were based upon ENDF/B-VI assuming that the fission and (n,2n) neutrons were isotropically emitted. That is only a qualitative assumption, but the corrections are not large. The corrected angle-integrated emission results generally agreed with the

scattering results to within several percent. This was considered reasonably good agreement given the uncertainties associated with the corrections to the emission distributions.

There are remarkably few previously reported experimental values comparable with the present results; all are quite old and all lack the detail of the present work. Knitter et al. [Kni+71] have reported scattering distributions up to ≈ 5 MeV but there are only a few values distributed over the range of scattering angles. Batchelor et al. [BGT65] have reported a 7 MeV distribution but, again without the detail of the present work. These previous results are qualitatively consistent with the present values but, because of their sparse nature, detailed quantitative comparisons with the present values are not rewarding.

IV. COUPLED-CHANNELS MODELS

The objective of the models was the provision of vehicles for the interpolation and extrapolation of the measured values. It was assumed that elemental uranium consisted entirely of the isotope ^{238}U and elemental thorium of the isotope ^{232}Th. Both targets were taken to be statically deformed rotors with the ground-state rotational band consisting of the yrast 0^+ g.s., 2^+ and 4^+ levels. The 6^+ and higher-lying levels of this band were ignored in the model considerations as their contributions to the observed scattering data are very small. The energies of the levels of the band were taken from the Nuclear Data Sheets [NDS]. No other levels contribute to the scattering observed in the present measurements. It is reasonable to expect strong coupling between these three members of the band. Therefore the model interpretations were carried out within the framework of the coupled-channels formalism, coupling the three levels together. It was further assumed that the incident energies of the present measurements were high enough so that only direct-reaction processes were contributing factors. This is a reasonable assumption as many channels are open, even at 4 MeV, and thus compound-nucleus contributions must be very small.

It was assumed that the real-potential of the model was of the Saxon-Woods form, that the absorption was confined to the nuclear surface and represented by an imaginary potential of the Saxon-Woods-derivative form, and that the spin-orbit potential was of the Thomas form [Hod71]. Throughout this effort the parameters of the spin-orbit potential were taken from work of Walter and Guss [WG86]. Volume absorption was not considered as the present measurements are at energies where it is generally not a concern. Both quadrupole (β_2) and hexadecapole (β_4) deformation parameters were used.

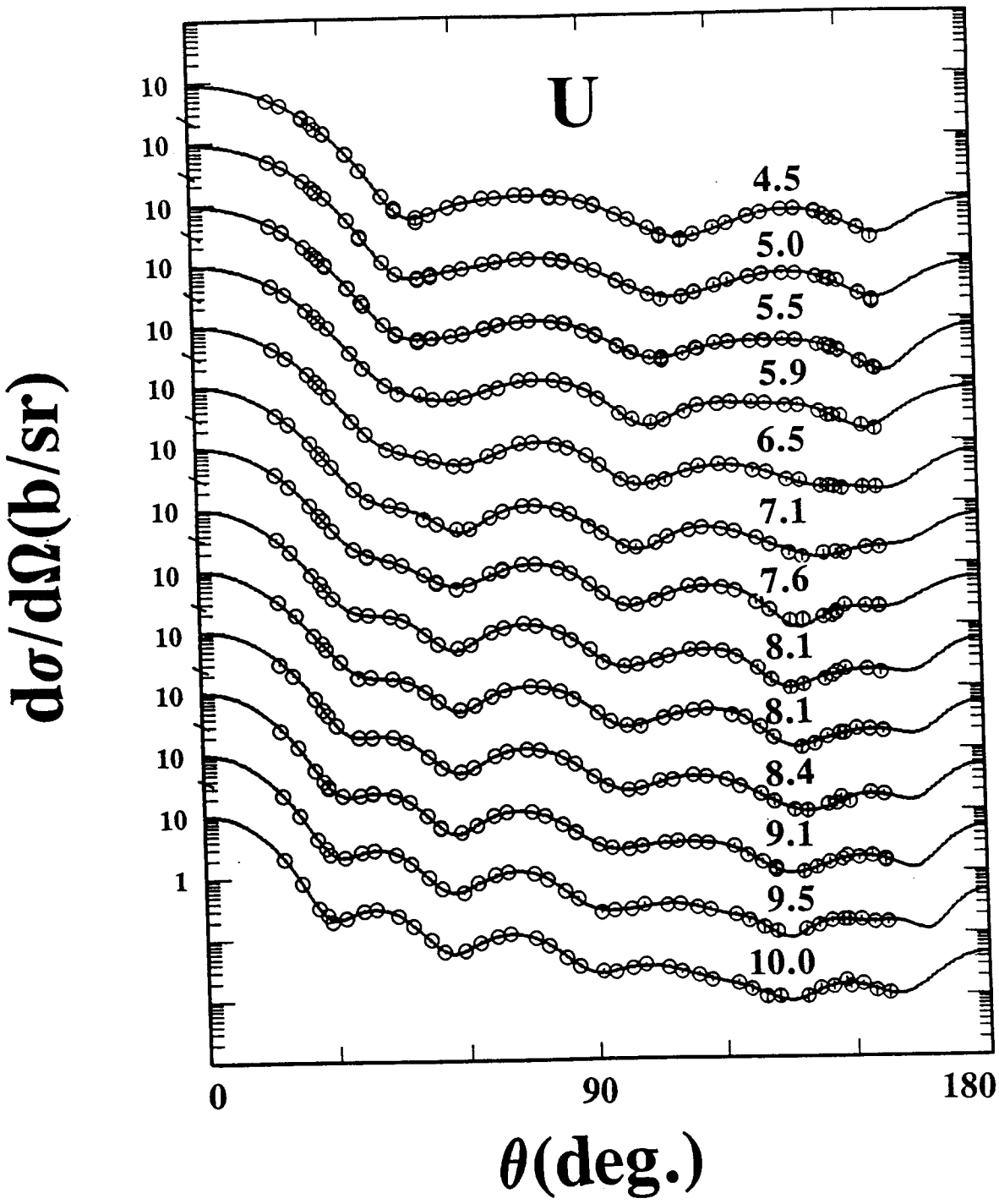

Fig.III-1. Uranium scattered-neutron distributions inclusive of 0^+, 2^+, 4^+ and 6^+ members of the ground-state rotational band. The measured values are indicated by symbols and the results of Legendre-polynomial fitting by curves. Approximate incident neutron energies are numerically noted in MeV. Throughout this work data are illustrated in the laboratory coordinate system.

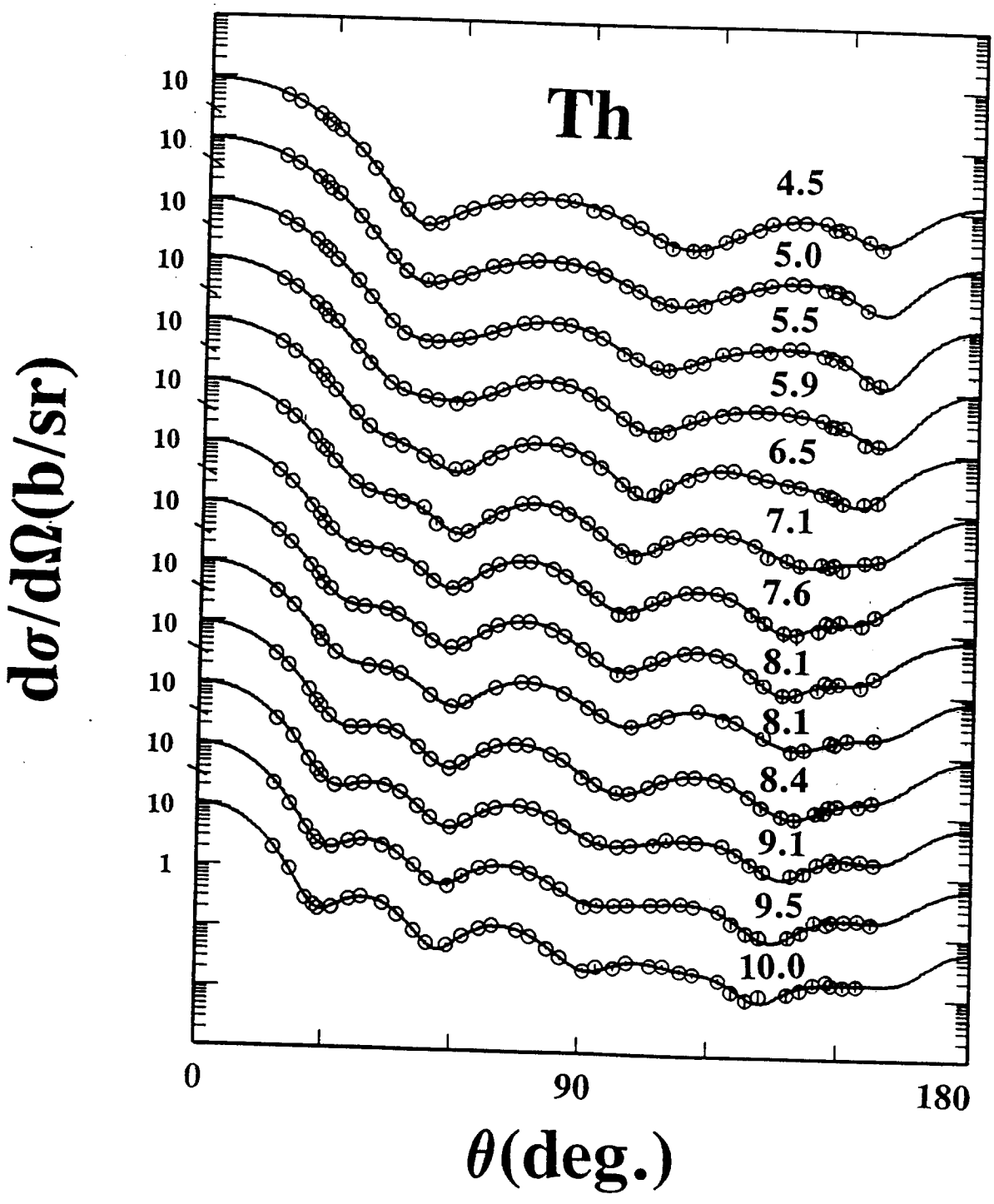

Fig. III-2. Thorium scattered-neutron distributions. The nomenclature is identical to that of Fig. III-1.

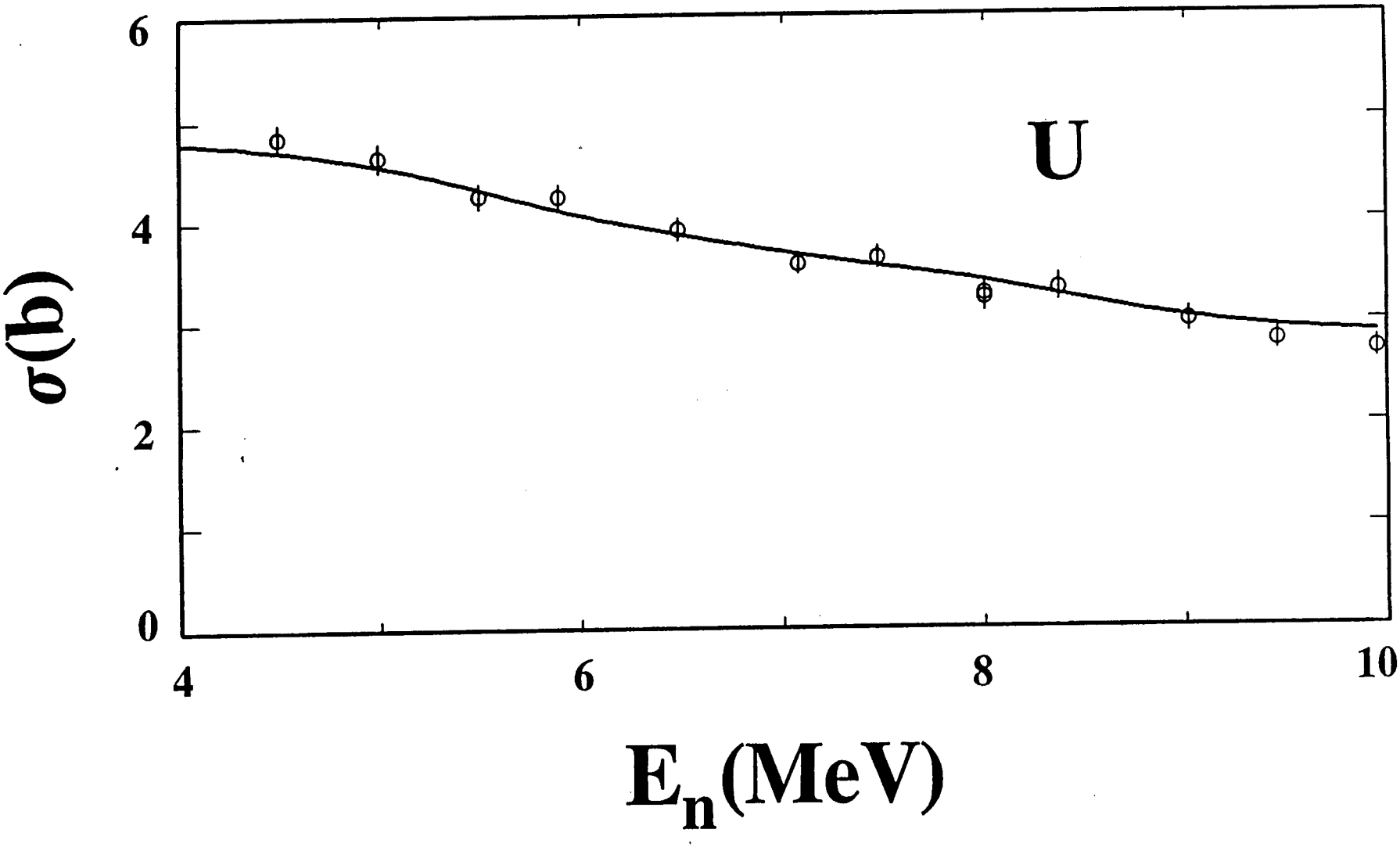

Fig. III-3. Uranium angle-integrated neutron-scattering cross sections. Symbols indicate the present experimental results and the curve the comparable values deduced from ENDF/B-VI.

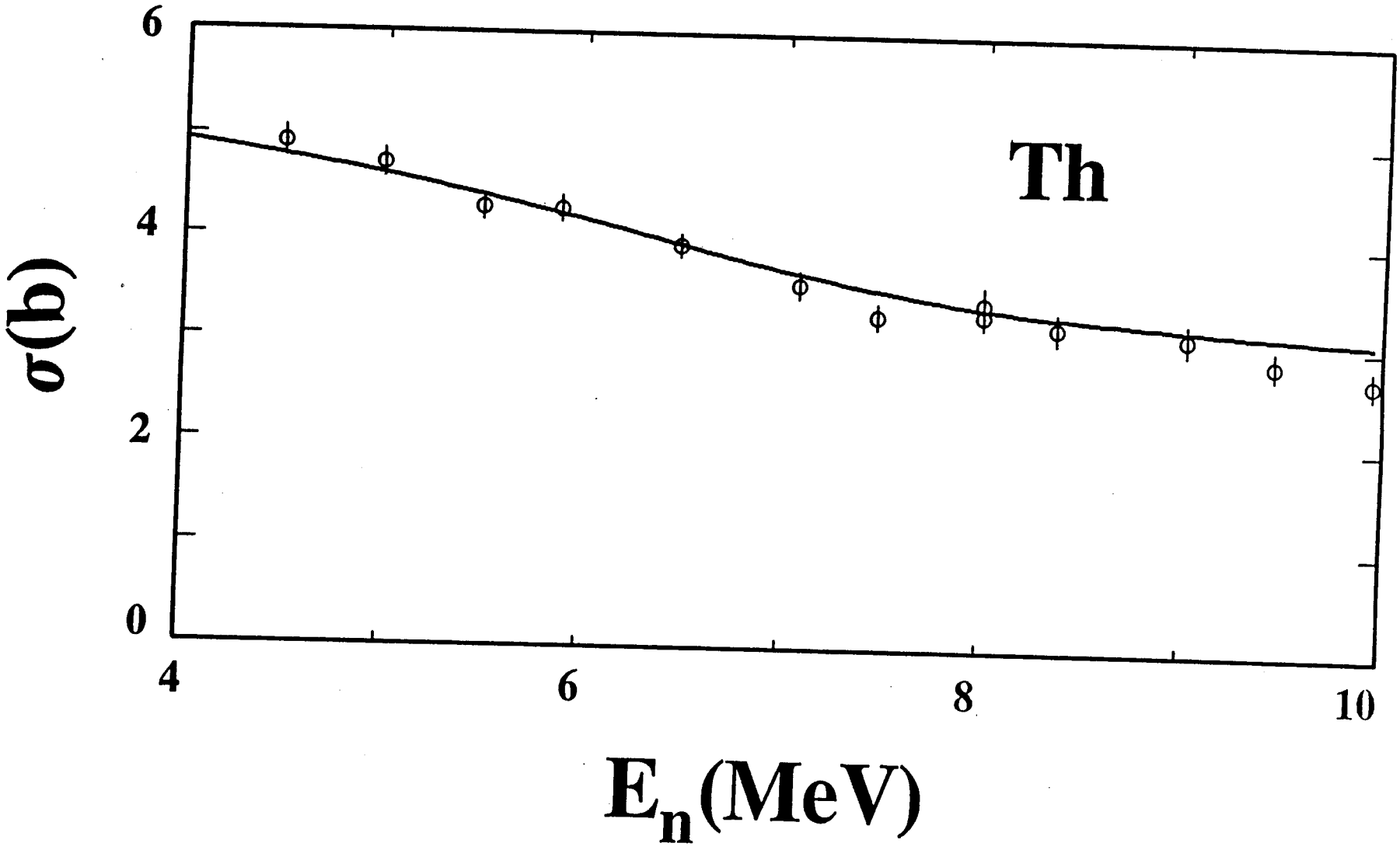

Fig. III-4. Thorium angle-integrated neutron scattering cross sections. The nomenclature is identical to that of Fig. III-3.

The real- and imaginary-potential parameters were deduced by explicitly chi-square fitting the present experimental results. The fitting procedure combined the elastic and first-two inelastic groups for determining chi-square so as to be consistent with the above-cited experimental resolutions. The fitting was pursued through five consecutive steps; i) From six-parameter fits varying real and imaginary strengths, radii and diffusenesses the real-potential diffuseness, a_v, was fixed. ii) Five parameter fits were used to fix the real-potential radius, r_v (herein the reduced radius is used, assuming that the actual radius $R_i \equiv r_i \cdot A^{1/3}$ where A is the target mass). iii) Four-parameter fits fixed the imaginary-potential radius, r_w. iv) Three parameter fits fixed the imaginary-potential diffuseness, a_w. and v) Finally, two-parameter fitting determined the real and imaginary potential strengths. This hierarchy of fitting has a weakness in that it is sensitive to the well know correlations of real-potential depth and radius, and of the imaginary-potential depth and diffuseness. This shortcoming should be mitigated by the extensive nature of the data base. On the other hand, the procedure avoids directing the result toward any pre-conceived region of parameter space. The fitting assumed that $\beta_2 = 0.216$ and $\beta_4 = 0.067$ for ^{238}U, and $\beta_2 = 0.206$ and $\beta_4 = 0.086$ for ^{232}Th. These are the values given by Lagrange [Lag75], based upon theoretical considerations. Somewhat different values can be found in the literature, but their use will have a small effect on the calculations, as noted below. The fitting procedure was tedious as the manipulation of many coupled equations is involved.

The resulting ^{238}U potential parameters are given in Table IV-1. The real-potential strength, J_v, falls with energy as illustrated in Fig. IV-1, though not as fast as frequently cited from equivalent-local Hartree-Fock calculations (throughout this work real- and imaginary-potential strengths are given as volume-integrals-per-nucleon). Concurrently, the imaginary strength, J_w, increases with energy as more channels open. These are, qualitatively, the expected energy dependencies of the strengths even though the data base from which they were developed is limited to six MeV and thus it is unreasonable to expect quantitative definition in a much wider energy scope. The ^{238}U potential of Table IV-1 gives a quite good description of the present experimental results, as illustrated in Fig. IV-2. Differences between measured and calculated values are appreciable only at the very large scattering angles where the calculations are more sensitive to the choice of the deformations and the spin-orbit potential, and where the experimental results are least reliable.

Table IV-1. ^{238}U Coupled-channels model parameters. Strengths, J_i, are given as volume-integrals-per-nucleon in units of MeV-fm^3, except for the spin-orbit strength which is given in MeV. Geometric parameters are given in fermis, and energies, E, in MeV.[a]

Real Potential

$J_v = 402.95 - 1.7844 \cdot E$

$r_v = 1.2342$

$a_v = 0.6558$

Imaginary Potential

$J_w = 23.261 + 3.0643 \cdot E$

$r_w = 1.2520$

$a_w = 0.6061$

Spin-orbit Potential

$V_{so} = 6.221 - 0.015 \cdot E$

$r_{so} = 1.103$

$a_{so} = 0.560$

Deformations

$\beta_2 = 0.216$

$\beta_4 = 0.067$

[a] Potential parameters are given to sufficient significant figures to permit accurate reproduction of the calculated results. The precisions do not necessarily imply uncertainties.

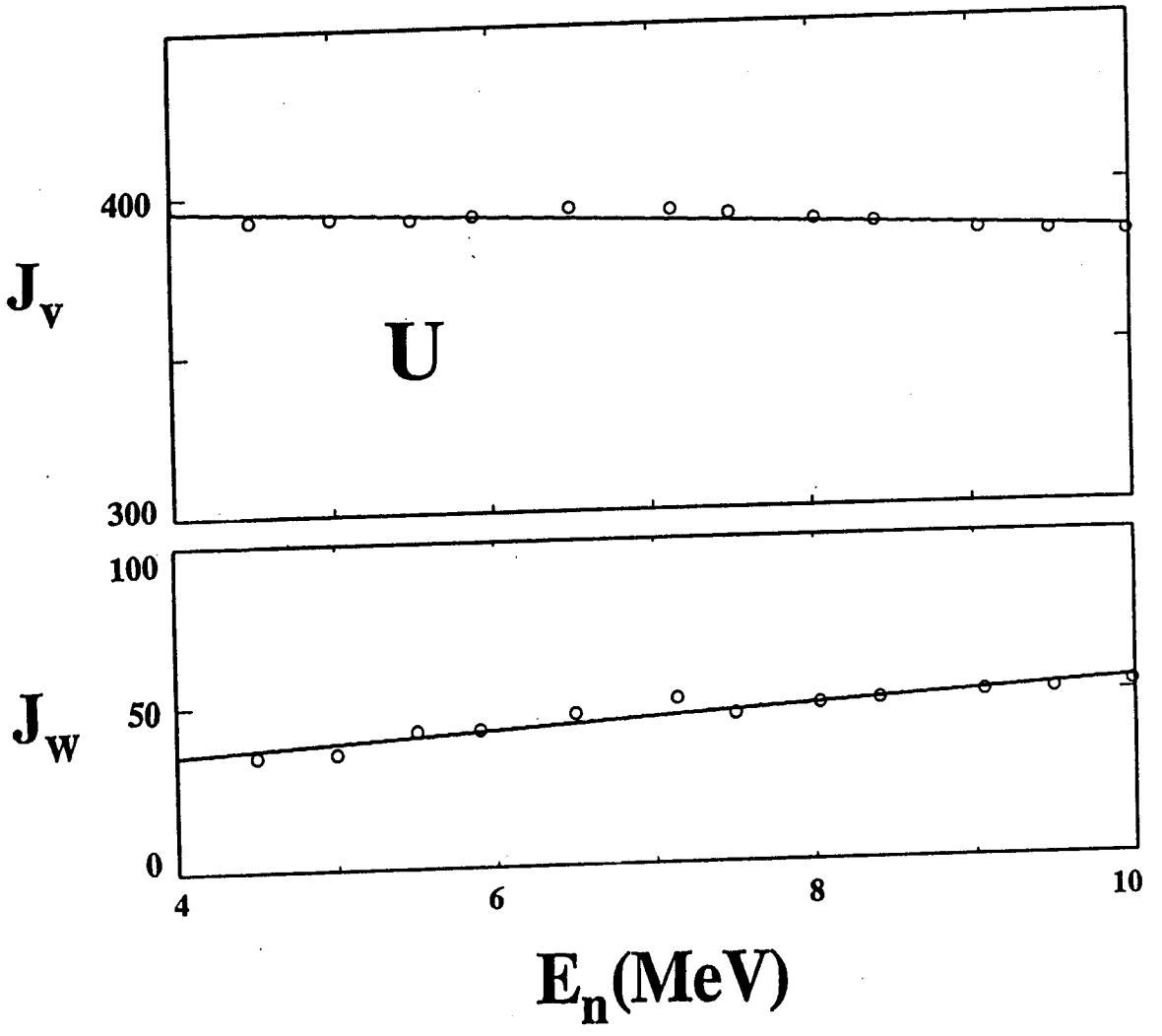

Fig. IV-1. Energy dependencies of the real, J_v, and imaginary, J_w, strengths of the ^{238}U model in units of MeV-fm^3. Symbols indicate the results obtained by fitting at the individual energies, and curves the linear parameterizations of Table IV-1.

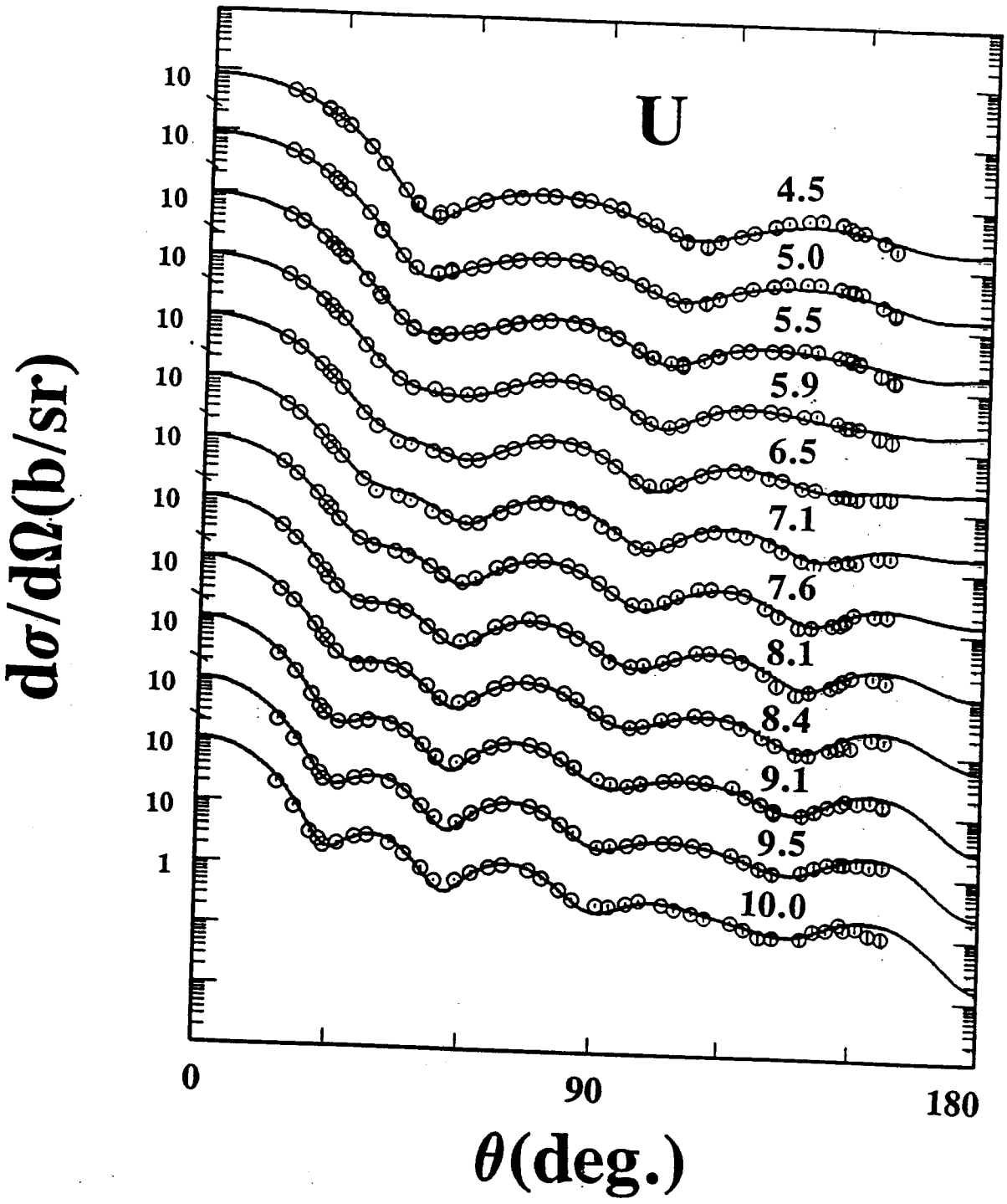

Fig. IV-2. Illustrative comparisons of measured and calculated ^{238}U scattered-neutron angular distributions. Symbols indicate the experimental results obtained in the present work and the curves the results of calculations using the potential of Table IV-1. Approximate incident-neutron energies are numerically noted in MeV.

The ^{232}Th potential derived from the fitting procedures is given in Table IV-2, and the energy dependencies of the real and imaginary strengths are illustrated in Fig. IV-3. Again, the model gives a reasonably good description of the measured values from which it was derived, as illustrated in Fig. IV-4. The ^{232}Th and ^{238}U real-potential strengths are nearly identical and the difference between the imaginary-potential strengths is reasonably good, particularly over the experimental energy range. Such similarity should be physically expected as the two potentials should differ by the product of the isovector strengths and the asymmetry parameter $\eta \equiv (N-Z)/A$. The latter is essentially identical for the two targets. There are some differences in the geometries of the two potentials but this is not surprising as geometries are strongly correlated with potential depths (as distinguished from potential strengths).

V DISCUSSION

Simple Legendre-polynomial fitting of the present uranium results leads to scattering cross sections for the combined excitation of the ground-state rotational band that are very similar to the comparable values given by ENDF/B-VI, as illustrated in Fig. III-3. Only one of the experimentally-deduced values differs from the comparable ENDF/B-VI quantity by more than the estimated uncertainty, and even then by a small amount. The scatter in the thorium angle-integrated values of the present measurements is larger than for the uranium case, but generally the experimentally-derived results are consistent with the comparable ENDF/B-VI values up to ≈ 9 MeV, as illustrated in Fig. III-4. At higher energies the experimental results are significantly lower than those given by ENDF/B-VI. This discrepancy is further supported by the model considerations discussed below. The above comments are relevant only to the scattering from the ground-state rotational band and, of course, do not identify the distribution of the components within the band.

The models of Section IV are explicitly applicable only to the limit range of the data from which they were derived (≈ 4 - 10 MeV). Within that scope they give a good description of the present experimental results, as illustrated in Figs. IV-2 and -4. The only significant discrepancies are at very large scattering angles. Calculated results in that angular region are largely governed by the contribution due to the excitation of the yrast 2^+ levels, as illustrated in Fig. V-1. The latter contribution can be varied by modifying the coupling strengths and/or the coupling scheme. The results are not particularly sensitive to variations in the β_i's. For example, 10% changes in

Table IV-2. ^{232}Th Coupled-channels model parameters. Strengths, J_i, are given as volume-integrals-per-nucleon in units of MeV-fm^3, except for the spin-orbit strength which is given in MeV. Geometric parameters are given in fermis, and energies, E, in MeV.[a]

Real Potential

$J_v = 402.27 - 1.9705 \cdot E$

$r_v = 1.2260$

$a_v = 0.6687$

Imaginary Potential

$J_w = 25.739 + 2.8475 \cdot E$

$r_w = 1.2852$

$a_w = 0.5666$

Spin-orbit Potential

$V_{so} = 6.221 - 0.015 \cdot E$

$r_{so} = 1.103$

$a_{so} = 0.560$

Deformations

$\beta_2 = 0.206$

$\beta_4 = 0.086$

[a] Potential parameters are given to sufficient significant figures to permit accurate reproduction of the calculated results. The precisions do not necessarily imply uncertainties.

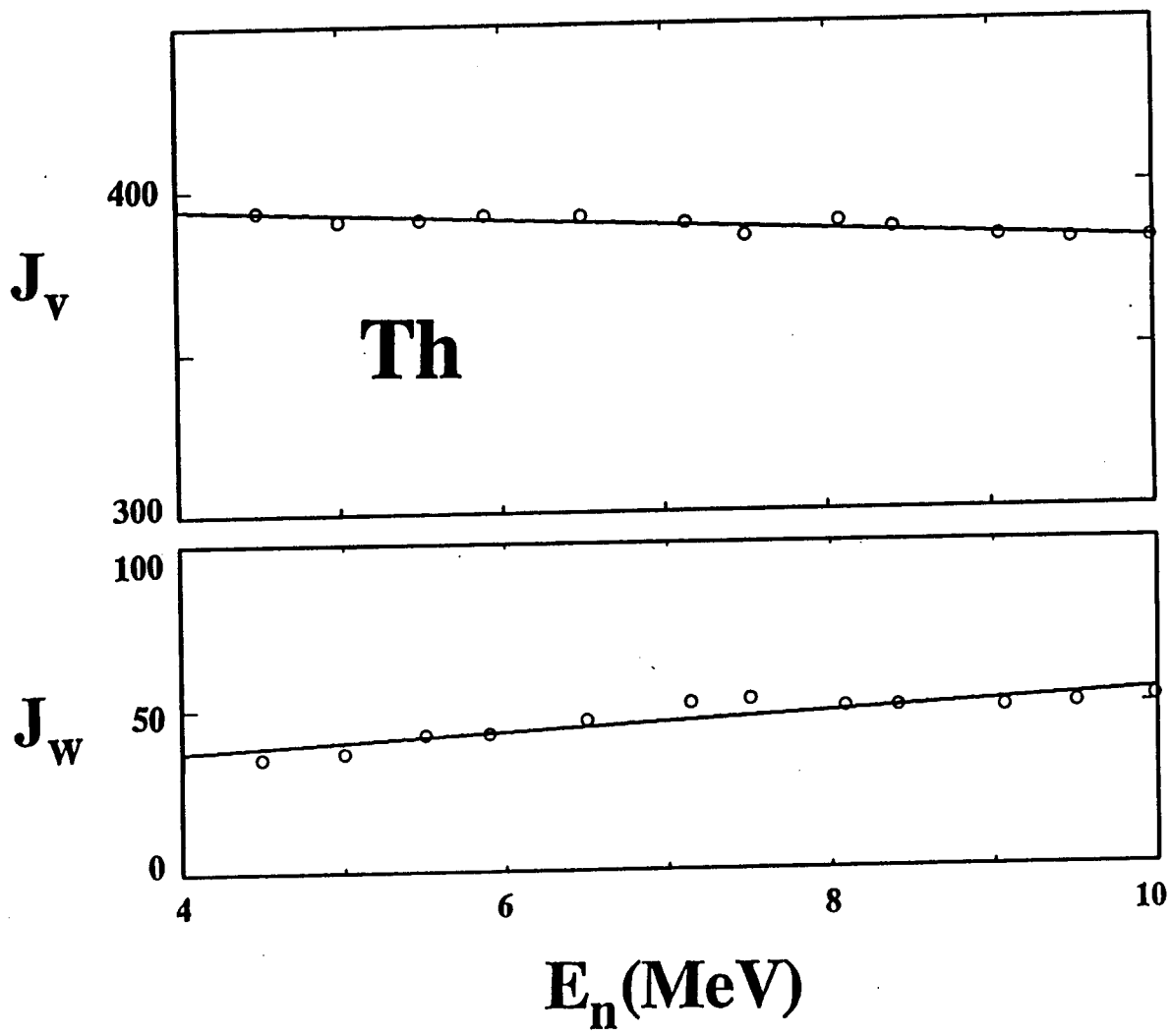

Fig. IV-3. Energy dependencies of the ^{232}Th real- and imaginary-potential strengths. The nomenclature is identical to that of Fig. IV-1.

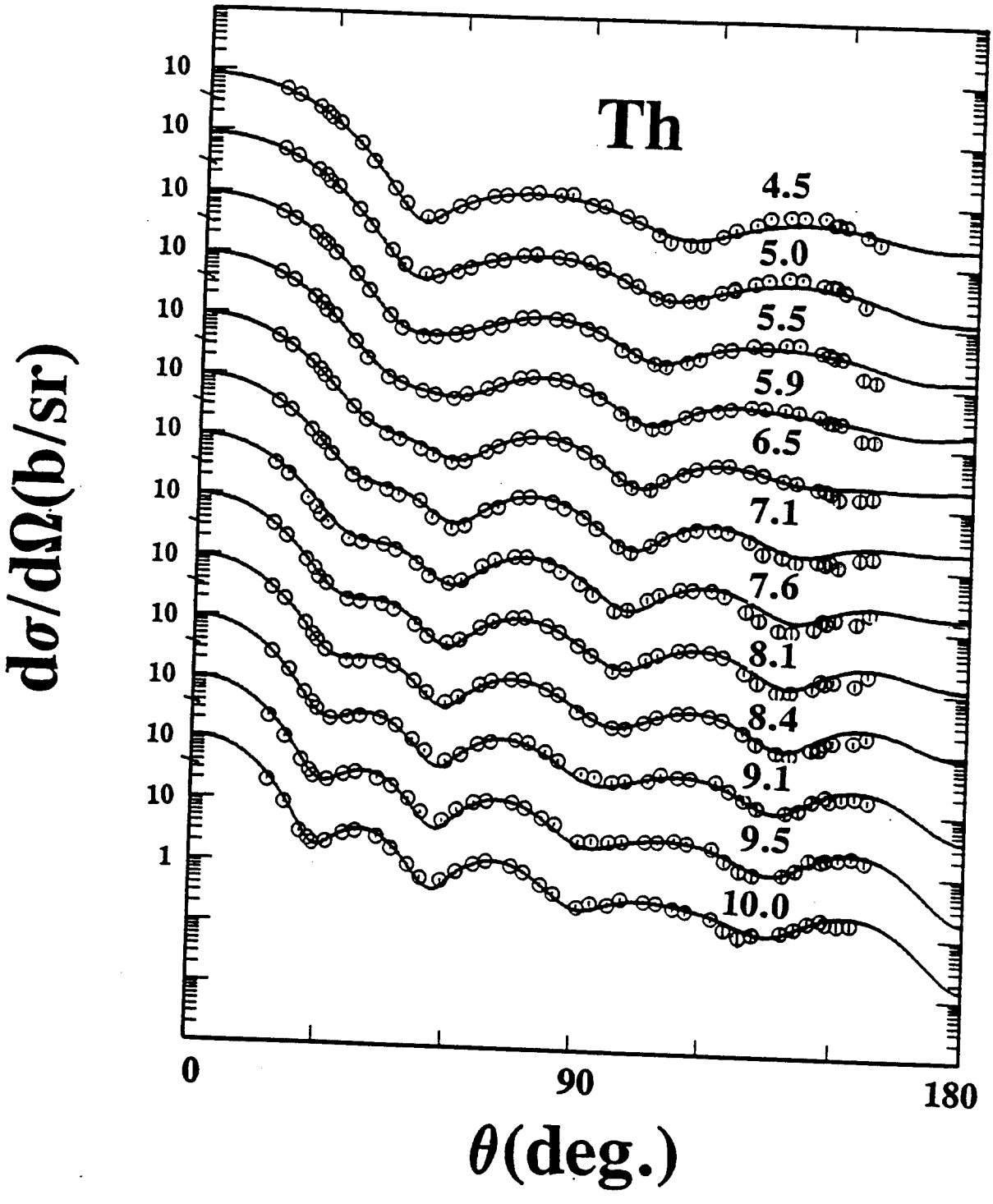

Fig. IV-4. Illustrative comparison of measured (symbols) and calculate (curves) ^{232}Th neutron-scattering cross sections. The nomenclature is identical to that of Fig. IV-2.

β_2 do not change the results of Fig. V-1 significantly outside the experimental uncertainties. Detailed studies of deformation strengths and/or coupling schemes in this energy range will be rewarding only when high-quality experimental information is available for each component of the band.

It is of interest to extrapolate the potentials to a wider energy range. The ^{238}U potential of Table IV-1 gives a reasonably-good description of the 14 MeV scattering results of Hansen et al. [Han+86], as shown in Fig. V-2. Going to lower energies, the potential gives a qualitative description of the 3.4 MeV elastic-scattering results of Haouat et al. [Hao+82], as illustrated in Fig. V-2. The latter measurements involve high resolutions and are very difficult. As a consequence, the measured values have some scatter. The potentials of Section IV can be further extrapolated to very low energies and used to calculate strength functions comparable with those deduced from resonance measurements. The results are given in Table V-1. In both the ^{232}Th and ^{238}U cases the calculated p-wave strength functions are very close to the experimentally-deduced values, while the calculated s-wave values are $\approx$ 15 - 45% larger than the experimentally-derived results. These are reasonably good agreements given the large energy extrapolation of the model and the fact that other work suggests that the imaginary-potential diffuseness becomes small as $E \rightarrow 0$ [Smi94], in contrast to approximately constant values at higher energies, and in the present interpretations.

The models of Section IV can also be used to extrapolate the present measurements to the individual reaction channels and thus to make detailed comparisons with ENDF/B-VI. Such an extrapolation for ^{238}U is summarized in Table V-2. The model gives total cross sections that differ from those of ENDF/B-VI by an average of 1.3%. That is very good agreement, even better than one should expect from the experimental uncertainties alone, though the ENDF/B values are systematically larger than those given by the model. The average deviation between ENDF/B elastic-scattering values and those projected by the model is $\approx$ 1.4%. Again, that is very good agreement, though there is some trend for the ENDF/B values to be systematically smaller about 5.7 MeV and larger about 7.5 MeV. This agreement implies that ENDF/B and the model result in very similar non-elastic and total-inelastic-scattering cross sections. The ENDF/B values for the inelastic excitation of the yrast 2^+ level are larger (by $\approx$ 10 - 15%) than the model predictions below $\approx$ 8 MeV, then become significantly smaller at 10 MeV. These differences amount to changes of as much as $\approx$ 50 mb which may be an applications concern. The ENDF/B values for the excitation of the yrast 4^+ level are generally larger than the model predictions by

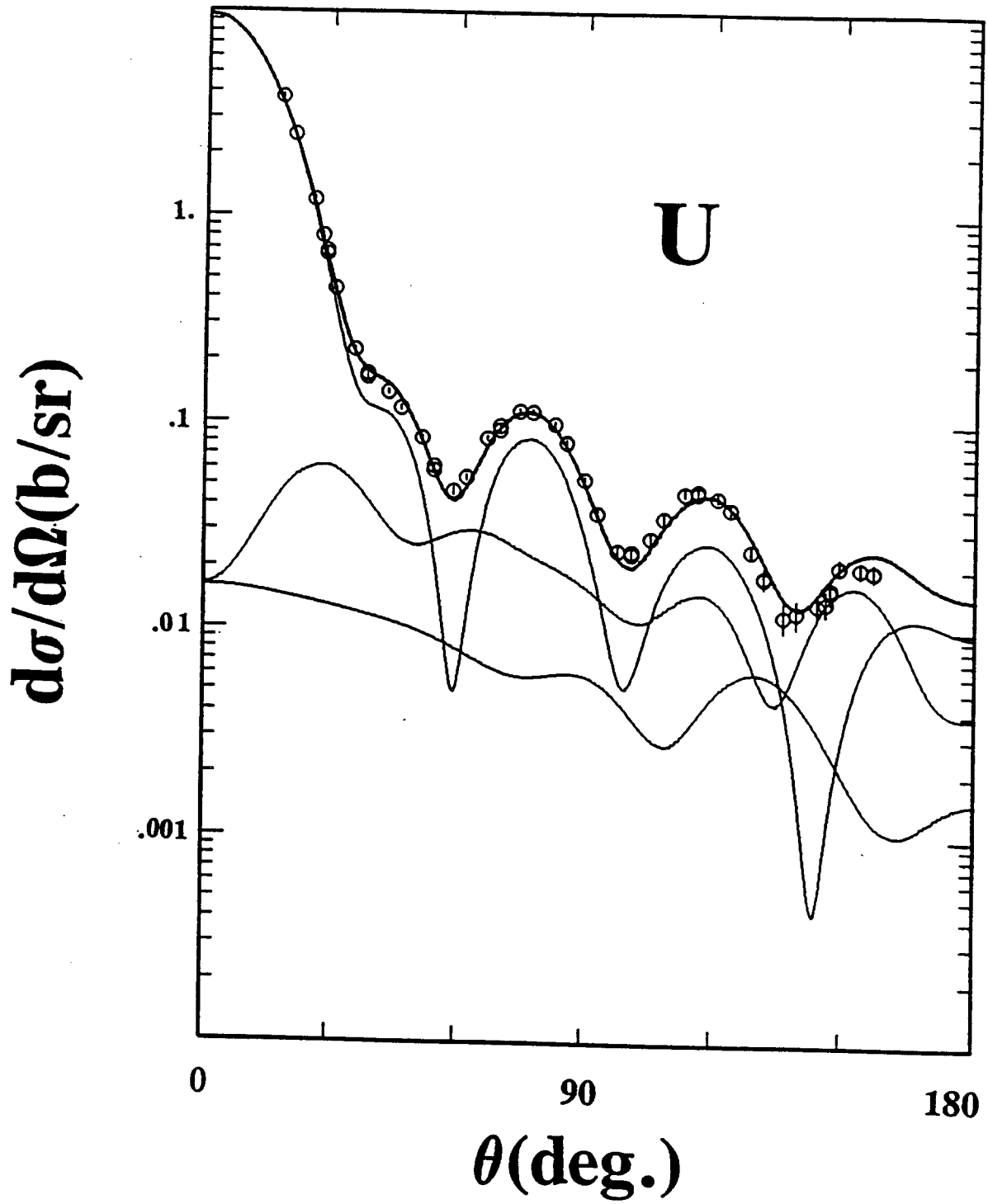

Fig. V-1. Measured and calculated ^{238}U neutron-scattering distributions at an incident energy of 7.5 MeV. Symbols indicate the present measurements. Curves denote the results of calculations where: i) the heavy curve is the composite result of scattering from the ground-state-rotational band, and the light curves represent ii) the elastic scattering, iii) next, scattering due to the excitation of the yrast 2^+ level, and iv) smallest, contributions due to the excitation of the yrast 4^+ level.

Table V-1. Strength functions in units of 10^{-4}.

Isotope	s-wave	p-wave
^{238}U		
Calculated (this work)	1.427	1.752
Experimental	1.2 ± 0.1[a]	1.7 ± 0.3[a]
	1.10 ± 0.05[b]	1.7 ± 0.2[b]
^{232}Th		
Calculated (this work)	1.511	1.651
Experimental	0.84 ± 0.07[a]	1.48 ± 0.07[a]

[a] S. Mughabghab, M. Divadeenam and N. Holden, Neutron Cross Sections (Academic, New York, 1981).

[b] Yu. V. Grigorev et al., IAEA Report, INDC(CCP)-372 (1994).

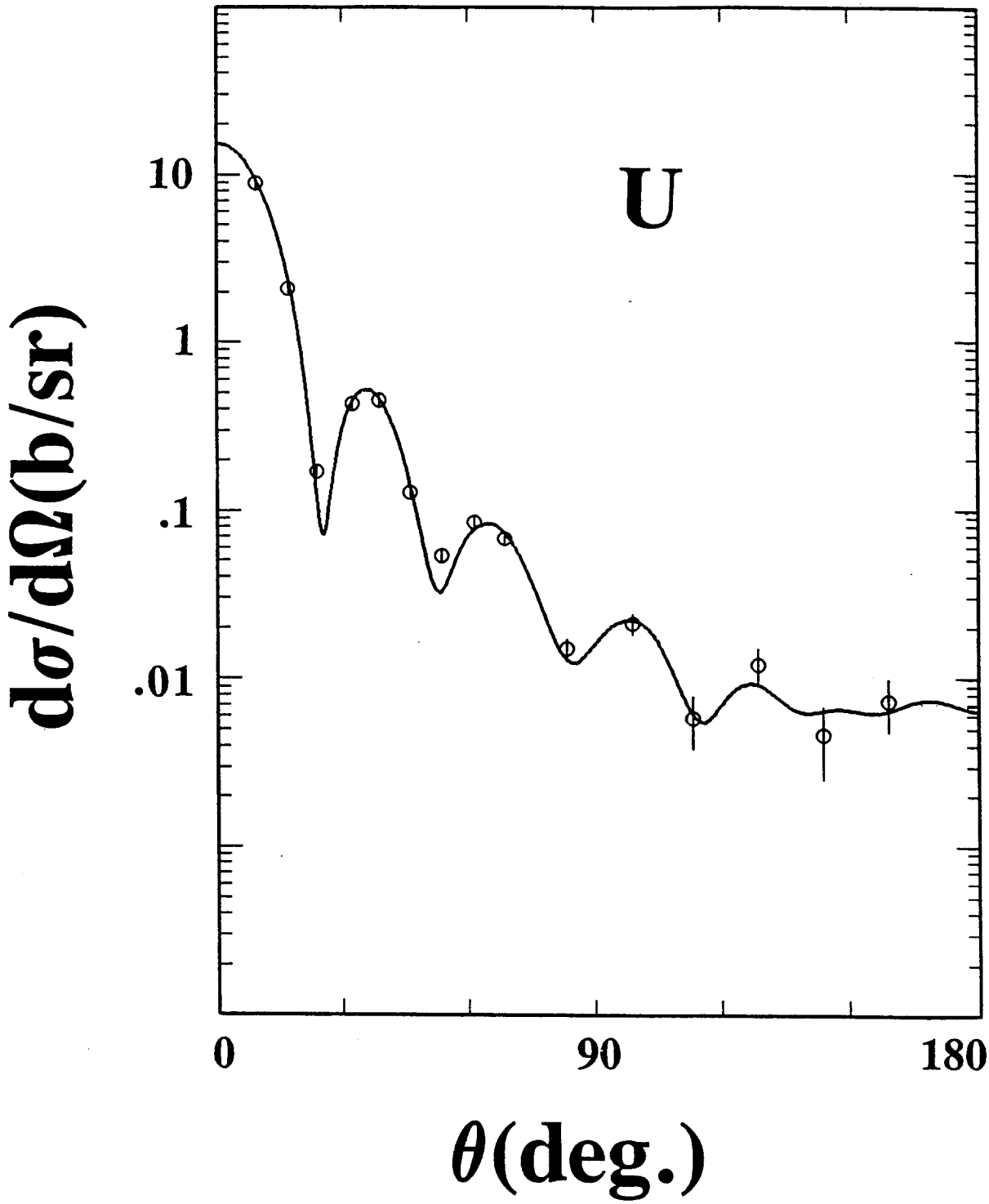

Fig. V-2. Comparison of measured and calculated ^{238}U scattering from the g.s. rotational band at 14 Mev. The experimental values of Hansen et al. [Han+86] are indicated by symbols and the curve denotes the result of calculation.

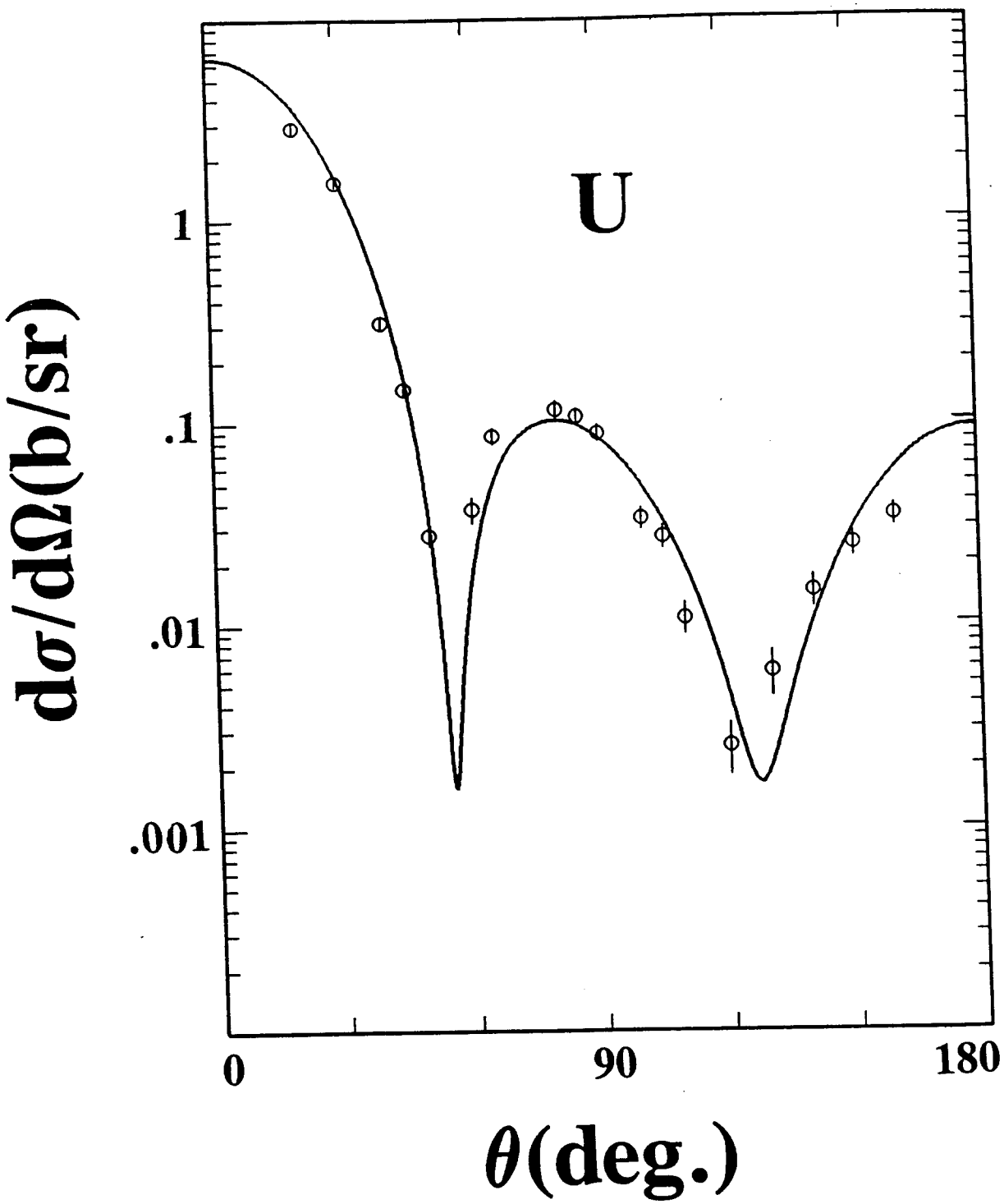

Fig. V-3. Comparison of measured and calculated ^{238}U elastic scattering at 3.4 MeV. The experimental values of Haouat et al. [Hao+82] are indicated by symbols and the result of calculation by the curve.

approximately 10%, except above ≈ 9 MeV where they become smaller. These are relatively large differences but the cross sections are small so the are cross-section differences are ≈ 10 mb or less, and that may not be of much concern in most applications.

Table V-3 makes similar comparisons between ENDF/B-VI ^{232}Th values and those suggested by the model. Again the ENDF/B and model total cross sections agree quit well, though the former appear to be systematically larger below 7 MeV and smaller above. The largest difference is only 2.3%. The elastic scattering of ENDF/B is larger than the model predictions over the entire energy range. The differences are relatively large, particularly above ≈ 8.5 MeV, and approach 10% at 10 MeV. This implies differences of ≈ 280 mb which may be an applied concern, and a consequence is that the ENDF/B and model non-elastic cross sections are significantly different. This is the same general trend noted in the simple Legendre-polynomial fitting shown in Fig. III-3. Below ≈ 8.5 MeV the ENDF/B cross sections for the excitation of the yrast 2^+ level are ≈ 20 - 25% larger than suggested by the model, or 75 - 100 mb. Those may be significant differences in some applications. The ENDF/B values for the excitation of the yrast 4^+ are much smaller than the model estimate throughout the energy range, reflecting differences of tens of mb's.

Generally, the present measurements and their model interpretation suggest some modest changes in the ENDF/B-VI ^{238}U file, particularly for the excitation of the yrast 2^+ below 8 MeV. For ^{232}Th the measurements and their model interpretation suggest significant changes in the ENDF/B-VI file in the areas of: i) elastic scattering, particularly above 8 MeV, ii) the excitation of the yrast 2^+ level over a wide energy range, and iii) considerable increases in the ENDF/B-VI cross sections for the excitation of the yrast 4^+ level.

ACKNOWLEDGEMENT

The authors are indebted to Dr. P. T. Guenther for his contributions to the early portions of this work.

Table V-2. Comparisons of ^{238}U evaluated and model-calculated cross sections. The evaluated cross sections are taken from ENDF/B-VI [ENDF]. The deviations between the evaluated and model-calculated results are given by $\delta \equiv$ (ENDF-Model)/ENDF. Energy, E_n, is given in MeV. Cross sections are noted by:- $\sigma_t \equiv$ total, $\sigma_{el} \equiv$ elastic scattering, $\sigma_{2+} \equiv$ inelastic scattering to the yrast 2^+ level, and $\sigma_{4+} \equiv$ inelastic scattering to the yrast 4^+ level. The reference cross-section values are taken from ENDF/B-VI.

E_n	σ_t(b)	δ(%)	σ_{el}(b)	δ(%)	σ_{2+}(b)	δ(%)	σ_{4+}(b)	δ(%)
4.50	7.853	+1.4	4.207	+0.2	0.395	+11.9	0.125	+8.8
5.00	7.659	+1.5	4.036	-0.8	0.380	+14.7	0.120	+10.0
5.50	7.422	+1.5	3.788	-2.7	0.363	+14.5	0.115	+11.3
5.90	7.225	+1.5	3.637	-2.6	0.349	+14.5	0.111	+11.8
6.50	6.922	+1.4	3.424	-1.8	0.330	+14.2	0.103	+11.7
7.14	6.649	+1.4	3.279	+1.3	0.310	+12.6	0.093	+9.7
7.55	6.505	+1.5	3.189	+3.1	0.296	+10.9	0.087	+9.1
8.06	6.344	+1.6	3.015	+2.7	0.278	+7.9	0.080	+6.3
8.41	6.242	+1.5	2.869	+0.8	0.266	+5.9	0.079	+4.1
9.06	6.072	+0.8	2.720	+0.1	0.243	+4.1	0.064	+3.1
9.50	5.983	+0.9	2.649	+0.0	0.228	-3.3	0.058	-5.2
10.0	5.915	+0.6	2.616	+0.6	0.210	-8.6	0.050	-16.0

Table V-3. Comparisons of ^{232}Th evaluated and model-calculated cross sections. The evaluated cross sections are taken from ENDF/B-VI [ENDF]. The deviations between the evaluated and model-calculated results are given by $\delta \equiv$ (ENDF-Model)/ENDF. Energy, E_n, is given in MeV. Cross sections are noted by:- $\sigma_t \equiv$ total, $\sigma_{el} \equiv$ elastic scattering, $\sigma_{2+} \equiv$ inelastic scattering to the yrast 2^+ level, and $\sigma_{4+} \equiv$ inelastic scattering to the yrast 4^+ level. The reference cross-section values are taken from ENDF/B-VI.

E_n	σ_t(b)	δ(%)	σ_{el}(b)	δ(%)	σ_{2+}(b)	δ(%)	σ_{4+}(b)	δ(%)
4.50	7.750	+1.2	4.374	+4.3	0.375	+21.1	0.063	-68.0
5.00	7.500	+0.3	4.173	+2.9	0.370	+22.4	0.060	-68.0
5.50	7.275	+0.3	3.981	+2.6	0.365	+24.4	0.055	-76.4
5.90	7.095	+0.4	3.821	+2.5	0.361	+25.5	0.051	-84.3
6.50	6.800	+0.3	3.541	+1.7	0.345	+24.9	0.045	-97.8
7.14	6.480	-0.4	3.292	+1.8	0.326	+23.3	0.039	-115.
7.55	6.275	-1.1	3.162	+2.2	0.314	+22.2	0.035	-131.
8.06	6.036	-2.3	3.014	+2.7	0.297	+23.2	0.030	-150.
8.41	5.956	-2.1	2.974	+4.4	0.278	+16.1	0.028	-161.
9.06	5.813	-2.0	2.904	+6.9	0.244	+7.8	0.025	-168.
9.50	5.760	-1.6	2.882	+8.5	0.221	+0.9	0.023	-178.
10.0	5.700	-1.2	2.857	+9.7	0.195	-12.3	0.020	-215.

REFERENCES

[Bar+66] E. Barnard, A. T. G. Ferguson, W. R. McMurray and I. J. Van Heerden, Nucl. Phys. 80 46 (1966).

[BGT65] R. Batchelor, W. B. Gilboy and J. H. Towle, Nucl. Phys. 65 236 (1965).

[BWS56] J. R. Beyster, M. Walt and E. Salmi, Phys. Rev. 104 1319 (1956).

[CL55] L. Cranberg and J. Levin, Proc. Inter. Conf. on Peaceful Uses of Atomic Energy (United Nations Press, New York, 1955).

[CSL83] Nuclear Standards File IAEA Report 227, eds. H. Conde, A. Smith and A. Lorenz (1983).

[Dro87] M. Drosg, IAEA Report, IAEA-TECDOC-410 (1987).

[Ega+88] J. J. Egan, A. Aliyar, C. A. Horton, G. R. Kegel and A. Mittler, Proc. Inter. Conf. on Nucl. Data for Sci. and Technology, ed. S. Igarasi, (Saikon Pub. Co. Ltd., Tokyo, 1988) p.-63.

[ENDF] Evaluated Nuclear Data File/B, Version VI, available from the National Nuclear Data Center, Brookhaven National Laboratory. Throughout this work citations of "ENDF/B" refer only to Version VI.

[Han+86] L. F. Hansen, B. A. Pohl, C. Wong, R. C. Haight and Ch. Lagrange, Phys. Rev. C34 2075 (1986).

[Hao+82] G. Haouat, J. Lachkar, Ch. Lagrange, Y. Patin and J. Sigaud, Nucl. Sci. Eng. 81 491 (1982)

[Hod71] P. E. Hodgson, Nuclear Reactions and Nuclear Structure (Clarendon, Oxford, 1971).

[Kni+71] H. H. Knitter, M. Coppola, N. Ahmed and B. Jay, Z. Phys. 244 358 (1971).

[Lag75] Ch. Lagrange, Proc. EANDC Topical Discussion on Critique of Models and Their Validity in the Evaluation of Nuclear Data, JAERI Report, JAERI-M-5984 (1975).

[Mol81] P. A. Moldauer, The coupled-channels computer code ANLECIS, private communication (1981); a modification of the ECIS code of J. Raynal [Ray79].

[NDS] M. R. Schmorak, Nucl. Data Sheets 36 367 (1982); E. N. Shurshikov, Nucl. Data Sheets 53 601 (1988).

[Ray79] J. Raynal, NEA memorandum (1979).

[Smi63] A. B. Smith, Nucl. Phys. 47 633 (1963).

[Smi+67] A. Smith, P. Guemther, R. Larson, C. Nelson, P. Walker and J. Whalen, Nucl. Instr. and Methods 50 277 (1967).

[Smi90] A. Smith, Argonne National Laboratory memorandum (1990) unpublished.

[Smi94] A. B. Smith, Argonne National Laboratory Report, ANL/NDM-133 (1994).

[SGM82] A. B. Smith, P. T. Guenther and R. D. McKnight, Proc. Inter. Conf. on Nuclear Data for Sci. and Technology, ed. K. H. Boeckhoff (Reidel Pub. Co., Dordrecht, Holland, 1982) p.-39.

[SGS77] A. B. Smith, P. T. Guenther and R. Sjoblum, Nucl. Instr. and Methods 140 397 (1977).

[SG90] A. Smith and P. Guenther, Argonne National Laboratory memorandum (1990) unpublished.

[Tam65] T. Tamura, Rev. Mod. Phys. 37 679 (1965).

[Wic43] G. C. Wick, Atti R. Accad. Ital. Memorie 13 1203 (1943).

[WG86] R. L. Walter and P. P. Guss, Proc. Conf. on Nucl. Data for Basic and Applied Science, eds. P. Young et al. (Gordon and Breach, New York, 1986) Vol. 2, p. 1079.

[YOM60] S. Yiftah, D. Okrent and P. A. Moldauer, Fast Reactor Cross Sections (Pergamon, New York, 1960).